Naunyn-Schmiedeberg's Archives of Pharmacology (2024) 397:5989–5999
https://doi.org/10.1007/s00210-024-03013-x

RESEARCH

Soat2 inhibitor avasimibe alleviates acute pancreatitis by suppressing acinar cell ferroptosis

Weiwei Luo[1,2] · Lin Chen[1,2] · Hui Sun[3] · Siqin Zhang[1,2] · Xiaowu Dong[1,2] · Jiajia Pan[4] · Weiming Xiao[1,2] · Guotao Lu[1,2] · Yaodong Wang[5] · Hongwei Xu[5]

Received: 12 October 2023 / Accepted: 13 February 2024 / Published online: 20 February 2024

Abstract

Ferroptosis, characterized by lipid peroxidation, plays a significant role in the pathogenesis of acute pancreatitis (AP). While sterol O-acyltransferase 2 (Soat2) is known for its crucial regulatory role in cholesterol homeostasis, its involvement in the development of AP remains unreported. We conducted this study to identify the pivotal role of Soat2 in AP using transcriptomic databases. Subsequently, we confirmed its alterations through both in vitro and in vivo experimental models. Furthermore, we performed intervention with the Soat2 inhibitor avasimibe to evaluate pancreatic tissue pathology and serum enzymatic levels and observe inflammatory cell infiltration through immunohistochemistry. Additionally, changes in indicators related to ferroptosis were also observed. The results showed that in the AP mouse model, the protein and mRNA levels of Soat2 were significantly increased. Following avasimibe administration, there was a decrease in serum amylase levels, reduction in pancreatic tissue pathological damage, and attenuation of inflammatory cell infiltration. Furthermore, avasimibe administration resulted in downregulation of ferroptosis-related indicators. In conclusion, our findings suggest that the Soat2 inhibitor avasimibe protects against AP in mice through inhibition of the ferroptosis.

Keywords Soat2 · Cholesterol metabolism · Avasimibe · Acute pancreatitis · Ferroptosis

Introduction

Acute pancreatitis (AP) is a common abdominal emergency characterized by both local and systemic inflammation, with varied clinical presentations. Most patients exhibit mild AP, which usually resolves spontaneously within a week, whereas approximately 20% of patients develop moderate or severe AP (Gardner 2021). The global incidence and mortality rates for AP were estimated to be 33.74 cases per 100,000 person-years and 1.60 deaths per 100,000 person-years, respectively (Xiao et al. 2016). Pancreatic tissue necrosis resulting from acinar cell injury is a significant contributor to disease progression (Schepers et al. 2019). Apoptosis, necroptosis, autophagy, and pyroptosis are different forms of regulated cell death (RCD) that play significant roles in the pathogenesis of AP (Li et al. 2022). Our previous studies have confirmed the significant involvement of ferroptosis, characterized by lipid peroxidation, in acinar cell injury (Ma et al. 2022).

In our previous study, we performed screening and co-analysis utilizing transcriptomic databases and the public GSE database (GSE109227). Through this analysis, we

Weiwei Luo, Lin Chen, and Hui Sun contributed equally to this work.

✉ Yaodong Wang
day.wang@live.cn

✉ Hongwei Xu
niannian5727@126.com

1 Department of Gastroenterology, Affiliated Hospital of Yangzhou University, Yangzhou University, Yangzhou, Jiangsu, China

2 Department of Gastroenterology, Pancreatic Center, The Affiliated Hospital of Yangzhou University, Yangzhou University, Yangzhou, Jiangsu, China

3 Department of General Surgery, Gaoyou People's Hospital, Yangzhou, Jiangsu, China

4 Department of Intensive Care, The Affiliated Hospital of Yangzhou University, Yangzhou University, Yangzhou, Jiangsu, China

5 Department of Gastroenterology, Kunshan Hospital of Traditional Chinese Medicine, Affiliated Hospital of Yangzhou University, Kunshan, Jiangsu, China

identified nine genes that exhibited upregulation in AP. One of these genes is sterol O-acyltransferase 2 (Soat2). Soat2 is an enzyme that facilitates the synthesis of cholesterol esters by esterifying free cholesterol and long-chain fatty acids within cells. It plays a crucial role in regulating the balance of cholesterol metabolism in the body (Ohtawa et al. 2018; Pramfalk et al. 2022). Furthermore, cholesterol metabolism has a regulatory influence on ferroptosis (Xu et al. 2020).

In this study, we focused on Soat2 and examined the role of its inhibitor, avasimibe, which was a novel orally available drug already on the market, in AP (Llaverias et al. 2003). This study presents a new perspective in the search for novel drugs for the clinical management of pancreatic necrosis.

Materials and methods

Animals

This study selected male wild-type (WT) C57BL/6 mice, purchased from the GemPharmatech Co. Ltd., Nanjing, China, weighing between 22 and 24 g. All mice were fed standard water and rodent feed freely, and a 12-h light/12-h dark cycle, at an environmental temperature of 25 °C ± 2 °C, and were raised without specific pathogen-free (SPF) conditions. All experiments were approved by the Scientific and Technological Committee of Affiliated Hospital of Yangzhou University.

Reagent

Caerulein (Cae) was purchased from Selleck Chem (S9690); cholecystokinin octapeptide (CCK-8) was purchased from Echelon Biosciences (471–47); amylase assay kit was purchased from BioSino (100,000,060); lipase assay kit was purchased from Nanjing Jiancheng Bioengineering Institute (A054-1–1); anti-GAPDH antibody was purchased from Santa Cruz Biotechnology (sc-32233); anti-GPX4 antibody was purchased from Abcam (ab125066); secondary antibodies against rabbit and mouse were purchased from Cell Signaling Technologies (7076 s, 7074 s); anti-F4/80 antibody was purchased from Servicebio (GB11027); anti-MPO antibody was purchased from Abcam (ab208670); avasimibe was purchased from MedChemExpress (HY-13215); PD128042 was purchased from TargetMol (114289–47-3); Triton X-100 was purchased from Beyetime (ST795); anti-amylise was purchased from Santa (sc46657); DAPI was purchased from Solarbio (S2110); Liproxstatin-1 (Lip-1) was purchased from MedChemExpress (HY-12726).

Methods

RNA-seq

Gene expression profiling analysis data was performed based on our own 266–6 cell transcriptome database and the public GSE database (GSE109227) (Withanage et al. 2022). R software was used for conducting the statistical analysis. PCA (principal component analysis) plots were employed for performing principal component analysis of the database. For the analysis of co-expressed genes, Venn diagrams were utilized. In addition, heat maps were utilized to display differentially expressed genes between two distinct groups.

Animal model establishment, grouping, and sample collection

Randomly divide the mice into control group, caerulein (Cae)-induced AP group, and avasimibe treatment groups with different concentrations (7.5 mg/kg, 15 mg/kg, 30 mg/kg). Except for the control group, all groups were intraperitoneally injected with Cae (200 μg/kg, intervals of 1 h, 10 times) to induce AP model. In the avasimibe treatment groups, avasimibe was administered 30 min after the first injection of Cae. Mice were euthanized 12 h after the first Cae injection. Anesthesia the mice and the pancreatic tissue was immediately collected. Half of the tissue samples were taken for pathological staining and immunohistochemical staining analysis. They were first fixed in 4% paraformaldehyde and then embedded, sliced, and stained the next day. The remaining tissues were quickly frozen in liquid nitrogen and stored at − 80° C for subsequent experiments.

Histological analysis

Pancreatic tissue was embedded and cut into 5-mm slices. The slices were stained with hematoxylin and eosin (H&E). Observation and photography of tissues were performed using a brightfield fluorescence microscope (BX53, Japan). The pancreatic pathology injury scores were evaluated based on tissue edema, acinar cell necrosis, and inflammatory cell infiltration according to the Schmidt method. The pathological scoring and analysis of the tissue were independently performed by two pathologists.

Immunohistochemistry

Cut the embedded pancreatic tissue into 5-mm sections and place them on a slide. Subsequently, the slide was dewaxed with xylene, dehydrated with anhydrous ethanol, and antigen-repaired with sodium citrate. By blocking endogenous

peroxidase and incubating with normal goat serum. The slides were then incubated overnight at 4 °C with anti-MPO antibody (diluted 1:200), anti-F4/80 antibody (diluted 1:100), and anti-GPX4 antibody (diluted 1:750). Biotinylated secondary antibodies were incubated for 1 h. The slides were stained using DAB chromogenic reagent, followed by a 10-min wash with tap water, counterstained with hematoxylin, dehydrated, and mounted with neutral resin. Tissue observations and photography were conducted under a microscope.

Western blot

Proteins from pancreatic tissue were extracted using the sonication method. Perform electrophoresis on the protein sample using 12% SDS-PAGE. After electrophoresis, transfer it to the PVDF membrane. Blocking with 5% skim milk and wash the membrane with TBST (3 times for 5 min each). Incubate the membrane overnight at 4 °C with the following primary antibodies: anti-Soat2 (diluted 1:200), anti-COX2 (diluted 1:1000), anti-GPX4 (diluted 1:1000), and anti-GAPDH (diluted 1:500). The next day, wash the membranes with TBST (3 times for 15 min each) and then incubate the corresponding second antibody for 2 h. Wash the membranes with TBST (3 times for 15 min each) and detect protein bands using the ECL Plus chemiluminescence system. Grayscale values of the images were measured using ImageJ software.

Amylase and lipase assay

We collected blood from the inner canthus of mice 6 h after the first injection of Cae, which can be temporarily stored at 4 ℃. Twelve hours after the first injection of Cae, collect mouse eyeball blood at 4000 r, centrifuge for 10 min, and then collect the serum. To make the measurement results more accurate, the serum was diluted appropriately. The serum obtained after 6 h was diluted 5 times, and the serum obtained after 12 h was diluted 10 times. Measure and calculate according to the manufacturer's instructions.

Pancreatic acinar cell (PAC) isolation and treatment

Pancreatic tissue was isolated from C57 mice and immediately digested using collagenase to obtain pancreatic acinar cells (PACs), as previously described (Hu et al. 2011). Culture the separated PACs in Hepes medium containing 4% fetal bovine serum. The PACs were incubated with varying concentrations of avasimibe (0.1, 0.5, 1, 5 μM) for 30 min and then treated with CCK (50 nM) as a cell injury model of AP for 6 h, observe cell morphology under microscope, and collect cells for subsequent experiments.

Immunofluorescence

The extracted PACs were cultured on cell climbing, broken cell membranes with 0.25% Triton X-100 for 15 min, and washed with PBS (3 times for 5 min each). Blocked with 5% goat serum for 1 h and then incubated overnight at 4 °C with primary antibody: anti amylase (1:250). The next day, the cell climbing was washed with PBS, and then the secondary antibody was incubated at room temperature in a dark environment for 2 h. DAPI stained the nucleus for 10 min and sealed with a cover glass slide and captured images using laser scanning confocal microscopy (×400).

PAC time point experiment

The collected PACs were incubated at 37 ℃ in Hepes medium containing 4% fetal bovine serum. CCK (50 nM) was used to construct a cell injury model of AP, and cells were collected after CCK treatment for 0 h, 1 h, 3 h, and 6 h, respectively. Wash cells with PBS to remove residual CCK; repeat 2–3 times. Add protein lysis buffer for extracting proteins, or add Trizol reagent to extract RNA from PACs.

Real-time reverse transcriptase-PCR (RT-PCR)

Total RNA from pancreatic tissues and PACs was extracted using the Trizol reagent (TIANGEN, DP424) following the manufacturer's instructions. cDNA was generated using a cDNA synthesis kit (Thermo Fisher Scientific, K1622). Real-time quantitative PCR was performed using SYBR Green PCR Master Mix (11201ES08, YEASEN) with the obtained cDNA as the template. Gene expression levels were quantitated using the comparative CT method, normalized to 18S. The following primer sequences were used:

18S F: GGAAGTGCACCACCAGGAGT
18S R: TGCAGCCCCGGACATCTAAG
Soat2 F: ACAAGACAGACCTCTTCCCTC
Soat2 R: ATGGTTCGGAAATGTTGCACC

Quantification of pancreatic acinar cell (PAC) injury in vitro

The lactate dehydrogenase (LDH) release experiment was detected by LDH Cytotoxicity Assay Kit (Beyotime, C0017). All procedures were conducted following the manufacturer's instructions.

MDA assay

The concentration of malondialdehyde (MDA), a product of lipid peroxidation, in the tissue was measured using the MDA assay kit. All procedures were performed according to the manufacturer's instructions.

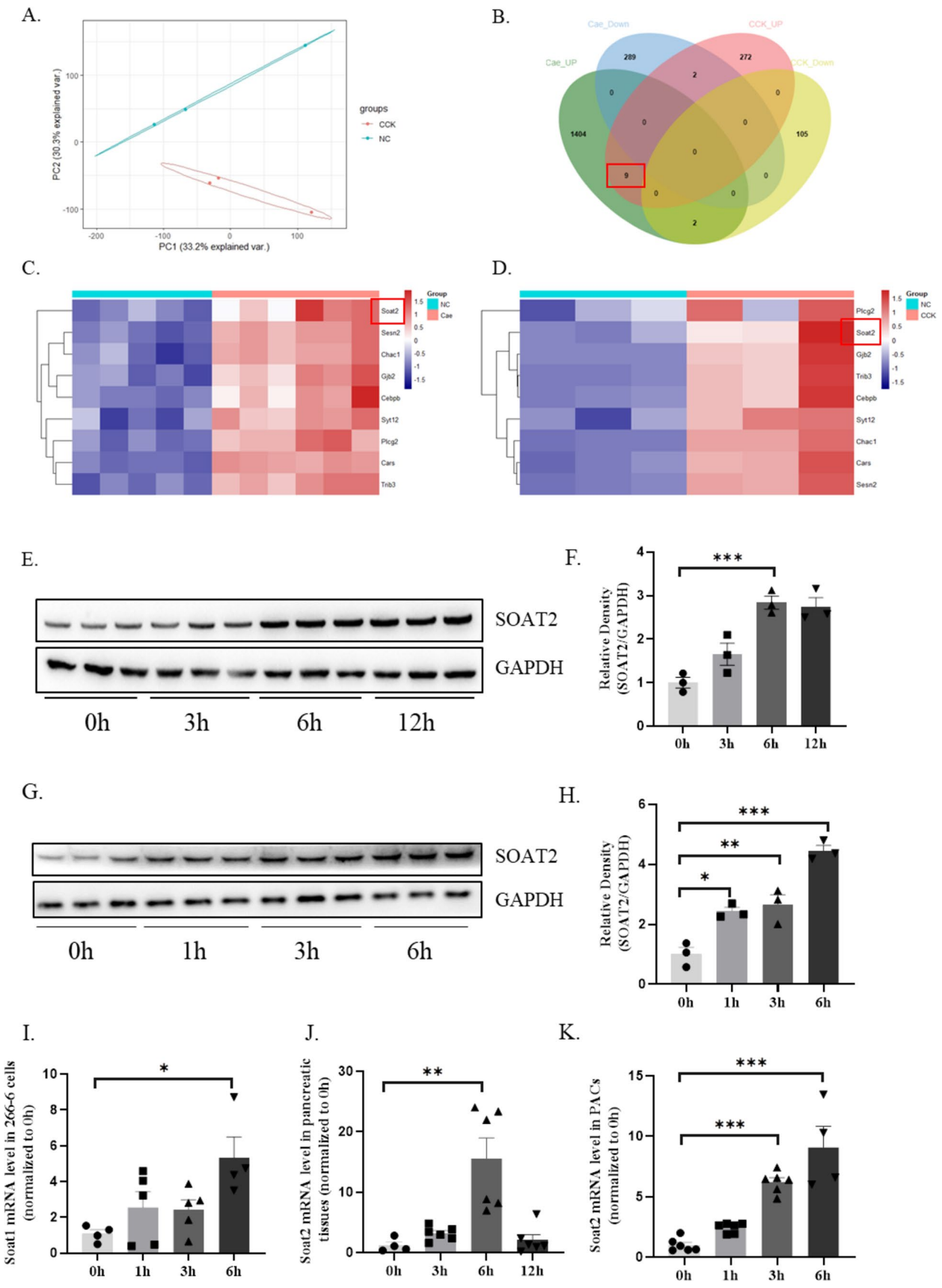
A.
PC2 (30.3% explained var.)
PC1 (33.2% explained var.)
groups
CCK
NC
B.
Cae_Down
CCK_UP
Cae_UP
CCK_Down
289
272
1404
105
9
C.
Group
NC
Cae
Soat2
Sesn2
Chac1
Gjb2
Cebpb
Syt12
Plcg2
Cars
Trib3
D.
Group
NC
CCK
Plcg2
Soat2
Gjb2
Trib3
Cebpb
Syt12
Chac1
Cars
Sesn2
E.
SOAT2
GAPDH
0h
3h
6h
12h
F.
Relative Density (SOAT2/GAPDH)
***
0h
3h
6h
12h
G.
SOAT2
GAPDH
0h
1h
3h
6h
H.
Relative Density (SOAT2/GAPDH)
***
**
*
0h
1h
3h
6h
I.
Soat1 mRNA level in 266-6 cells (normalized to 0h)
*
0h
1h
3h
6h
J.
Soat2 mRNA level in pancreatic tissues (normalized to 0h)
**
0h
3h
6h
12h
K.
Soat2 mRNA level in PACs (normalized to 0h)
***
***
0h
1h
3h
6h

◂**Fig. 1** Soat2 was significantly overexpressed in the AP model in mice. **A** Principal component analysis (PCA) of the transcriptome database of 266–6 cells. **B** Co-expression analysis of the 266–6 cell transcriptome database with the public GSE database (GSE109227). **C** Heatmap showing significant changes in the Soat2 gene in the mouse AP model. **D** Heatmap showing significant changes in the Soat2 gene in the 266–6 cell injury model. **E** Protein levels of Soat2 were analyzed in pancreatic tissue by western blotting (WB) after induction of mouse AP model at different time points using caerulein. **F** Relative protein expression of Soat2, GAPDH was used as a control for protein loading. **G** Protein levels of Soat2 were analyzed in pancreatic acinar cells (PACs) by WB after inducing the injury model at different time points using CCK. **H** Relative protein expression of Soat2. **I** The mRNA expression of Soat2 was detected in 266–6 cells in vitro by RT-PCR. **J** The mRNA expression of Soat2 was detected in pancreatic tissues in vivo by RT-PCR. **K** The mRNA expression of Soat2 was detected in PACs in vitro by RT-PCR. $n = 4$ each group. $^{*}p < 0.05$, $^{**}p < 0.01$, and $^{***}p < 0.001$

Statistical analysis

Quantitative data are presented as mean ± standard error of the mean (SEM), and bar graphs depict mean ± SEM. The comparison between two groups was performed using the *t*-test, while the comparison among three or more groups, following a normal distribution, was conducted using one-way analysis of variance (ANOVA). GraphPad Prism 8.0 software was used for data analysis and graphing. Statistical significance was considered significant if $p < 0.05$.

Results

Transcriptomic analysis of AP revealed significant overexpression of the Soat2 gene

We induced an in vitro injury model of 266–6 cells using CCK and collected cells at 0 and 6 h for transcriptomic analysis. We performed PCA on the obtained 266–6 cell transcriptome database (Fig. 1A) and correlated it with the public GSE database (GSE109227). We found that nine genes, including Soat2, were upregulated in AP (Fig. 1B). This public database is an animal model induced by caerulein. Heatmap analysis (Fig. 1C) revealed significant differences in Soat2 gene expression in pancreatic tissue of the AP mice model compared to the normal control group. Similarly, significant differences were observed in the CCK-induced 266–6 cell in vitro injury model (Fig. 1D).

An AP model was induced in mice using caerulein, and WB analysis was performed to observe changes in the expression of the Soat2 protein in pancreatic tissue at different time points. The results showed that Soat2 expression was weak in normal pancreatic tissue, while it was significantly increased in the pancreatic tissue of AP mice (Fig. 1E). Pancreatic acinar cells (PACs) were extracted and cultured, and cell purity was observed using immunofluorescence (Fig. S1A). Then, WB analysis was performed in the CCK-induced injury model of PACs, similar conclusions were obtained (Fig. 1G). Furthermore, mRNA levels of Soat2 were validated using qPCR, and changes were observed at different time points. The validation results are shown in Fig. 1I–K. The CCK-induced 266–6 cell in vitro injury model, caerulein-induced in vivo AP model in mice, and CCK-induced PAC in vitro injury model were used. The results demonstrated significant increases in the mRNA levels of Soat2 in the AP model. In summary, in vitro and in vivo models, we observed the changes and trends of Soat2 with disease progression through experiments at different time points.

These findings suggest that Soat2 may play an important regulatory role in the occurrence and progression of AP. However, further research is still needed to explore the specific functions and mechanisms of Soat2 in AP.

The Soat2 inhibitor avasimibe alleviates caerulein-induced AP in mice

To further elucidate the role of Soat2 in AP in mice, we established a PAC injury model using CCK and incubated the cells with different concentrations of the Soat2 inhibitor avasimibe, as well as a control vehicle. The release of LDH in the cell culture supernatant was measured. The result demonstrated that treatment with avasimibe led to a dose-dependent attenuation of acinar cell necrosis, as depicted in Fig. 2A. Furthermore, we employed an additional Soat2 inhibitor, PD128042, in the PAC injury model. Likewise, we administered different concentrations of PD128042 externally and measured the release of LDH in the cell culture supernatant. The result showed that PD128042 demonstrated a protective effect against acinar cell necrosis (Fig. 2B). These findings further confirm the role of Soat2 in the development of AP. Meanwhile, the drug toxicity of the two inhibitors in PACs was observed by measuring LDH release (Fig. S1B, C).

Subsequently, we established a mouse AP model using caerulein and evaluated the effects of avasimibe treatment on this model. The experimental results showed that avasimibe pretreatment significantly reduced the histological manifestations of pancreatic injury compared to the AP group (Fig. 2C). These features included decreased infiltration of inflammatory cells, alleviated edema, and alleviated extent of necrosis (Fig. 2F, I). In addition, the serum levels of amylase and lipase also significantly decreased in the avasimibe-treated group (Fig. 3D, E) (Fig. S2A–F). Furthermore, through immunohistochemical analysis, we evaluated the infiltration of inflammatory cells in pancreatic tissue (neutrophils marked by MPO and macrophages marked by F4/80). The results showed that avasimibe alleviated inflammation infiltration

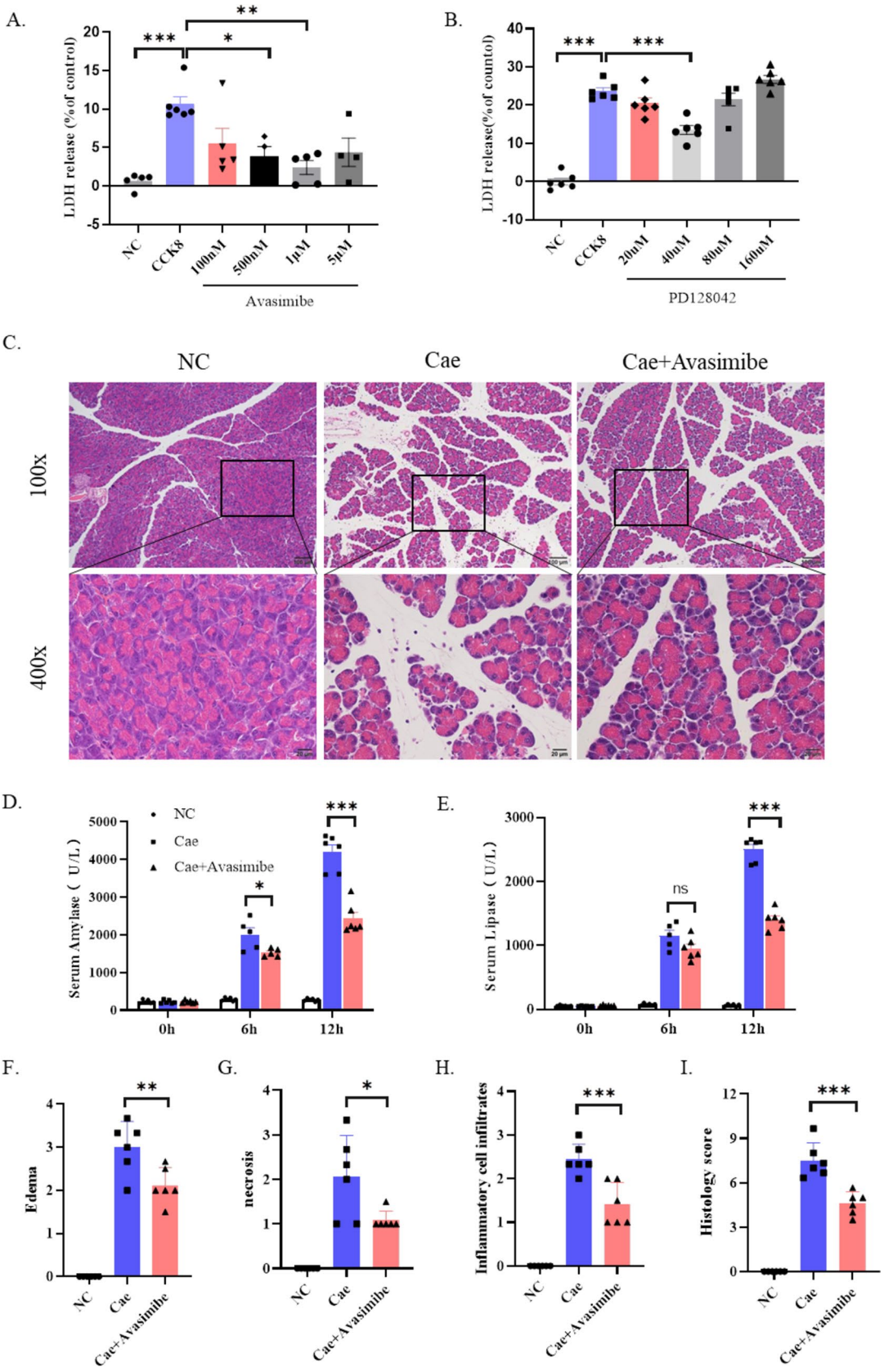
A.
LDH release (%of control)
NC
CCK8
100nM
500nM
1μM
5μM
Avasimibe
B.
LDH release(%of countol)
NC
CCK8
20uM
40uM
80uM
160uM
PD128042
C.
NC
Cae
Cae+Avasimibe
100x
400x
D.
Serum Amylase (U/L)
NC
Cae
Cae+Avasimibe
0h
6h
12h
E.
Serum Lipase (U/L)
ns
F.
Edema
G.
necrosis
H.
Inflammatory cell infiltrates
I.
Histology score

◂**Fig. 2** Avasimibe alleviates the severity of caerulein-induced AP in mice. **A** LDH release of PACs stimulated with 50 nM CCK8 6 h and different concentrations of avasimibe. **B** LDH release of PACs stimulated with 50 nM CCK8 6 h and different concentrations of PD128042. **C** Representative HE stains of pancreatic tissues in magnifications × 100 and × 400. **D**, **E** Serum levels of amylase and lipase. **F–I** Histopathological scores of pancreatic tissue (edema, inflammation, necrosis). $n = 7$ each group. $^{*}p < 0.05$, $^{**}p < 0.01$, and $^{***}p < 0.001$. Cae, caerulein. Cae + avasimibe (30 mg/kg)

(Fig. 3A–C). In conclusion, the results demonstrate that avasimibe, a Soat2 inhibitor, effectively improves the severity of the cerulein-induced AP model in mice.

Avasimibe alleviates AP by inhibiting ferroptosis pathway

Liproxstatin-1 (Lip-1) was used as a specific ferroptosis inhibitor. Previous study in our laboratory showed that CCK-induced ferroptotic cell death was inhibited by Lip-1 (Ma et al. 2022). Primary pancreatic acinar cells (PACs) derived from C57 mice were stimulated with CCK and incubated with or without avasimibe (1 μM) and Lip-1 (5 μM). LDH in the cell culture supernatant was measured (Fig. 4A). The result indicated that avasimibe can alleviate CCK-induced cell damage. However, under the premise of inhibiting acinar cell ferroptosis with Lip-1, administration of avasimibe did not further alleviate CCK-induced cell damage. This indicated that avasimibe alleviates acute pancreatitis by suppressing acinar cell ferroptosis.

Next, we examined indicators associated with ferroptosis. Figure 4B shows the results of WB analysis; we observed an increase in COX2 protein expression in pancreatic tissue after 12 h of AP induction, but decreased following avasimibe treatment. Conversely, glutathione peroxidase 4 (GPX4) protein expression decreased following AP induction, but increased after treatment with avasimibe. This indicated that avasimibe inhibits the ferroptosis pathway. Furthermore, immunohistochemical staining results showed that under normal conditions, the expression of GPX4 protein was primarily localized in the cytoplasm of acinar cells, which significantly decreased after the onset of AP. However, following the administration of avasimibe, a significant increase in GPX4 expression was observed (Fig. 4F, G). Additionally, we measured the concentration of malondialdehyde (MDA), a lipid peroxidation product, in pancreatic tissue (Fig. 4E). The experimental results showed that avasimibe treatment effectively reduced the level of lipid peroxidation in pancreatic tissue, thereby alleviating lipid peroxidation.

Discussion

AP is a common digestive emergency with a high mortality rate, particularly when it develops into severe AP (James and Crockett 2018). Currently, the lack of specific therapeutic targets is a major contributing factor to the high mortality rate. Over the last decade, a substantial amount of research has been conducted to comprehending the pathophysiological mechanisms of AP (Lee and Papachristou 2019). Inhibition of lipid peroxidation has been considered a potential therapeutic approach to prevent severe damage in AP (Altavilla et al. 2003). This study highlights our demonstration of the efficacy of avasimibe, an effective inhibitor of Soat2, can alleviate acinar cell necrosis and improve the severity of AP in mice by inhibiting the ferroptosis pathway. These findings suggest that Soat2 could serve as a promising target for future preventative and therapeutic interventions for AP in a clinical context.

Soat2 is the only enzyme in cells that catalyzes the formation of cholesterol esters from free cholesterol and long-chain fatty acids. It plays a crucial role in maintaining the balance of cholesterol metabolism in the body (Wang et al. 2017; Pramfalk et al. 2022). Research has demonstrated that the natural elevation of total cholesterol (TC) levels in plasma during pregnancy can render fetal blood vessels vulnerable to oxidative stress, leading to an augmented likelihood of maternal–fetal complications, such as acute pancreatitis (Mauri et al. 2021). A case–control study discovered a notable association between the occurrence of AP and cholesterol concentration in the plasma (Shen et al. 2021). Additionally, non-alcoholic fatty liver disease (NAFLD) is an independent risk factor for AP. Existing research has established that NAFLD can exacerbate AP by promoting bacterial translocation and perturbing cholesterol metabolism in the liver and pancreas (Lin et al. 2022). Therefore, Soat2 could potentially play a role in the pathogenesis of AP by modulating cholesterol metabolism. Through an analysis of transcriptomic databases, we discovered substantial overexpression of Soat2 in AP. To authenticate these findings, we established an in vivo model of PACs injury and an in vitro mouse model of AP. Subsequently, we performed comprehensive experiments at both the RNA and protein levels. The results showed that Soat2 was significantly upregulated in AP. These findings contribute to a deeper understanding of the pivotal role played by Soat2 in the pathogenesis of AP.

Avasimibe, an effective orally active inhibitor of Soat2, exerts a protective effect in numerous inflammatory diseases (Delsing et al. 2001; Raal et al. 2003; Hu et al. 2017). Due to its demonstrated good and safe anti-inflammatory properties in humans, it has entered the

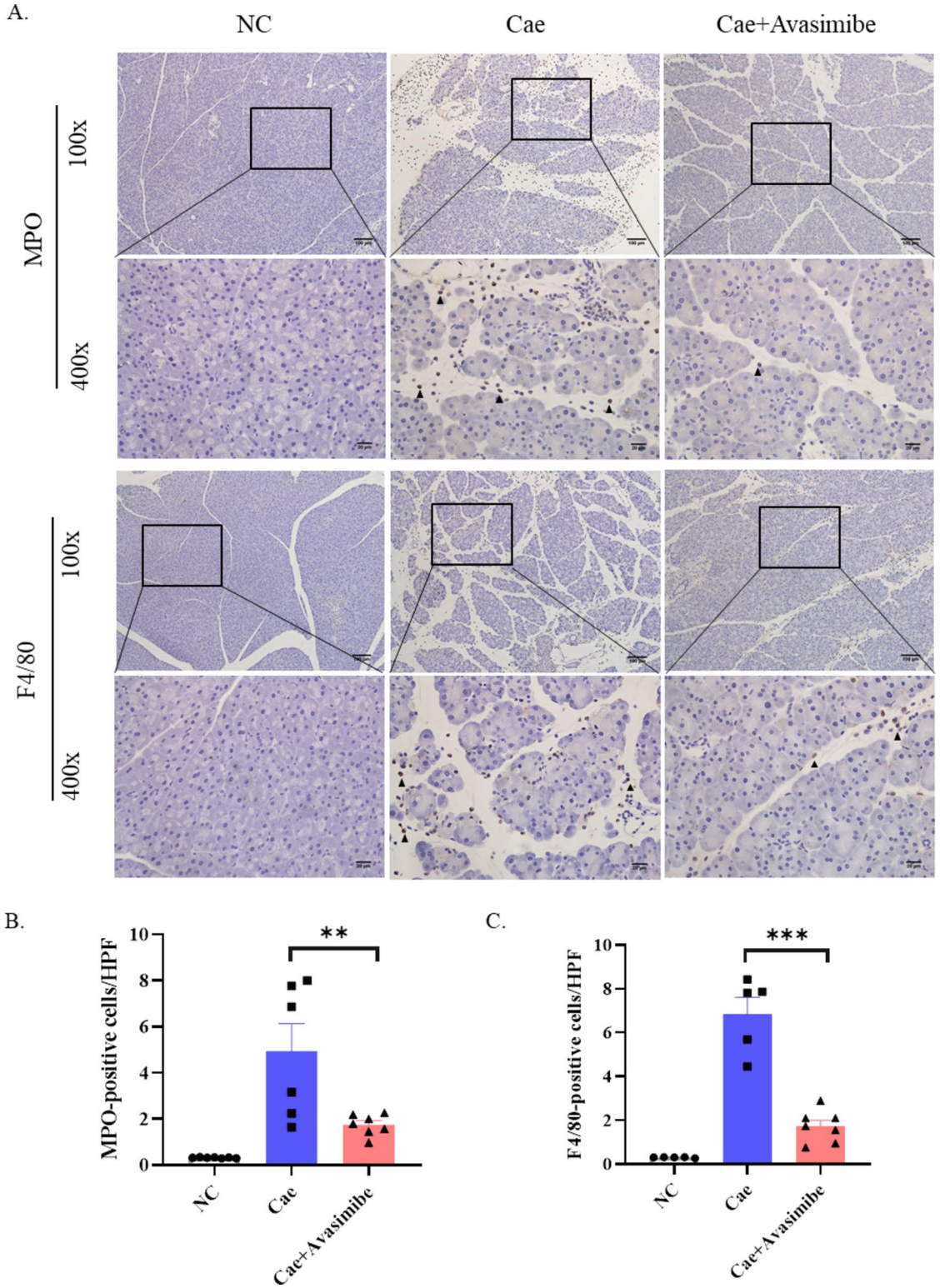

Fig. 3 Avasimibe prevents the infiltration of immune cells in the pancreatic tissues of mice. **A** Representative immunohistochemical images of MPO and F4/80 in the pancreas, magnifications × 100 and × 400, with black arrows to indicate positive staining. **B** Quantification of MPO positive cells. **C** Quantification of F4/80 positive cell. ($n = 6$ each group). $^{*}p < 0.05$, $^{**}p < 0.01$, and $^{***}p < 0.001$. Cae, caerulein, Cae + avasimibe (30 mg/kg)

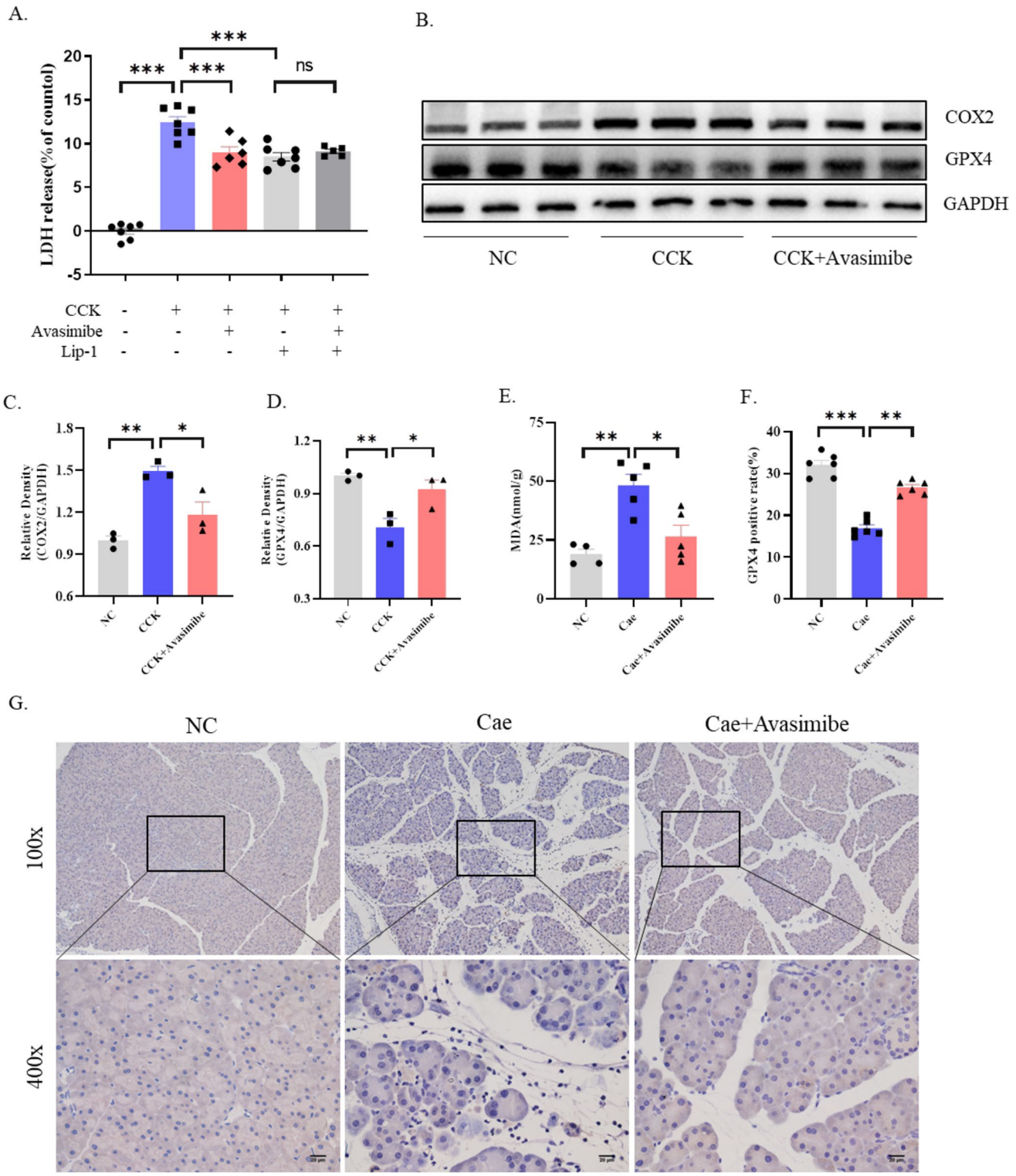

Fig. 4 Avasimibe alleviates AP by inhibiting the ferroptosis pathway. **A** LDH release of PACs stimulated with 50 nM CCK8 6 h and incubated with or without avasimibe (1 μM) and Lip-1 (5 μM). **B** Protein levels of COX2 and GPX4 in PACs were analyzed by WB. **C**, **D** Relative protein expression of COX2 and GPX4, GAPDH was used as a control for protein loading. **E** Effects of avasimibe on the malondialdehyde (MDA) as an indicator of oxidative damage in the pancreatic tissue. **F** Quantification of the GPX4 positivity rate. **G** Representative immunohistochemistry images of GPX4 in the pancreas, magnifications × 100 and × 400. ($n = 6$ each group). *$p < 0.05$, **$p < 0.01$, and ***$p < 0.001$. Cae, caerulein, Cae + avasimibe (30 mg/kg)

clinical trial stage for the treatment of atherosclerosis (Llaverias et al. 2003). Recent studies have also found that Avasimibe can effectively alleviate the disruption of the airway epithelial barrier, potentially becoming a new treatment option for allergic asthma (Zhou et al. 2022). In addition, Avasimibe has shown anti-tumor effects in various cancers, with great potential for application (Huang et al. 2017; Goudarzi 2019; Liu et al. 2022). In this study, using an in vitro model of PAC injury, we observed a reduction in LDH release with avasimibe treatment, suggesting a protective effect of Soat2 inhibition on AP. We observed that 5 μM avasimibe and high concentration of PD128042 caused the increase in LDH, indicating that the drug's effect continues to enhance with increasing dose, but exceeding a certain range can produce toxic side effects of the drug. The LDH trend in the PD128042 group is different from that in the avasimibe group because they are inhibitors of different classes. Furthermore, we observed significant protective effects of avasimibe on AP in an animal model, mainly manifested as alleviation of pancreatic tissue pathological damage, reduction in serum amylase and lipase levels, and decreased infiltration of inflammatory cells in pancreatic tissue. These findings suggest that avasimibe confers protection against pancreatic injury in mice with AP.

Ferroptosis was a novel programmed cell death process characterized by lipid peroxidation and the accumulation of iron. These events are primarily caused by reduced glutathione levels, inactivation of GPX4, and lipid toxicity (Friedmann Angeli et al. 2014; Hirschhorn and Stockwell 2019). GPX4 is a crucial enzyme involved in lipid peroxidation. Our previous studies have shown that specific knockdown of GPX4 expression in the pancreatic cell line 266–6 can lead to high levels of lipid peroxidation and increased cell death (Ma et al. 2022). The GPX4-dependent ferroptotic process plays a vital role in acute pancreatitis. Recent studies have indicated that the *Mikania micrantha* extract can improve hypercholesterolemia and lipid peroxidation by inhibiting Soat2 in a high-cholesterol diet–induced rat model (Ibrahim et al. 2020). Furthermore, cholesterol metabolism also plays an important role in regulating ferroptosis in tumors (Xu et al. 2020). However, there have been no reports on the role of Soat2-regulated cholesterol metabolism in ferroptosis during AP. To investigate this issue, immunohistochemistry staining and WB were conducted to analyze the expression changes of GPX4 and the level of MDA, a product of lipid peroxidation, in pancreatic tissues. The results showed that treatment with the Soat2 inhibitor avasimibe led to an increase in GPX4 expression in pancreatic tissues. In addition, it was observed that the expression of COX2 and MDA was suppressed. These findings suggest that avasimibe exerts a protective effect against AP by inhibiting the ferroptotic process. This study provides important supplementary information for understanding the role of cholesterol metabolism in the regulation of ferroptosis during AP.

Supplementary Information The online version contains supplementary material available at https://doi.org/10.1007/s00210-024-03013-x.

Author contributions HWX, YDW, and WMX contributed to the study idea and critical experimental design; WWL, LC, HS, and SQZ acquired, analyzed, and interpreted the data; WWL and JJP wrote the initial manuscript; XWD and GTL revised and approved the final review of the manuscript. All authors gave their final approval to the submitted version. The authors declare that all data were generated in-house and that no paper mill was used.

Funding This work was supported by National Natural Science Foundation of China (no. 82070668, no. 82270680 and no. 82200720); Yangzhou City Policy Guidance Program (International Science and Technology Cooperation) Project (no. YZ2022207); Yangzhou Key Research and Development Program (Social Development) Project (no. YZ2022080).

Data availability All data supporting the findings of this study are available within the paper and its Supplementary Information.

Declarations

Ethical approval The experimental procedures were implemented in accordance with the Guide for the Care and Use of Laboratory Animals. All animal experiments were approved by the Ethics Committee of Yangzhou University (Approval No. 202210013).

Competing interests The authors declare no competing interests.

References

Altavilla D, Famulari C, Passaniti M, Campo GM, Macri A, Seminara P, Marini H, Calo M, Santamaria LB, Bono D, Venuti FS, Mioni C, Leone S, Guarini S, Squadrito F (2003) Lipid peroxidation inhibition reduces NF-kappaB activation and attenuates cerulein-induced pancreatitis. Free Radic Res 37:425–435

Delsing DJM, Offerman EH, van Duyvenvoorde W, van der Boom H, de Wit ECM, Gijbels MJJ, van der Laarse A, Jukema JW, Havekes LM, Princen HMG (2001) Acyl-CoA: cholesterol acyltransferase inhibitor avasimibe reduces atherosclerosis in addition to its cholesterol-lowering effect in ApoE*3-Leiden mice. Circulation 103:1778–1786

Friedmann Angeli JP, Schneider M, Proneth B, Tyurina YY, Tyurin VA, Hammond VJ, Herbach N, Aichler M, Walch A, Eggenhofer E, Basavarajappa D, Radmark O, Kobayashi S, Seibt T, Beck H, Neff F, Esposito I, Wanke R, Forster H, Yefremova O, Heinrichmeyer M, Bornkamm GW, Geissler EK, Thomas SB, Stockwell BR, O'Donnell VB, Kagan VE, Schick JA, Conrad M (2014) Inactivation of the ferroptosis regulator Gpx4 triggers acute renal failure in mice. Nat Cell Biol 16:1180–1191

Gardner TB (2021) Acute pancreatitis. Ann Intern Med 174:ITC17–ITC32

Goudarzi A (2019) The recent insights into the function of ACAT1: a possible anti-cancer therapeutic target. Life Sci 232:116592

Hirschhorn T, Stockwell BR (2019) The development of the concept of ferroptosis. Free Radic Biol Med 133:130–143

Hu GY, Shen JQ, Cheng L, Guo CY, Xu XF, Wang F, Huang L, Yang LJ, He M, Xiang D, Zhu SY, Wu MY, Yu Y, Han W, Wang XP (2011) Reg4 protects against acinar cell necrosis in experimental pancreatitis. Gut 60:820–828

Hu LB, Li JQ, Cai H, Yao WX, Xiao J, Li YP, Qiu X, Xia HM, Peng T (2017) Avasimibe: a novel hepatitis C virus inhibitor that targets the assembly of infectious viral particles. Antivir Res 148:5–14

Huang Y, Jin Q, Su M, Ji F, Wang N, Zhong C, Jiang Y, Liu Y, Zhang Z, Yang J, Wei L, Chen T, Li B (2017) Leptin promotes the migration and invasion of breast cancer cells by upregulating ACAT2. Cell Oncol (dordr) 40:537–547

Ibrahim A, Shafie NH, Mohd Esa N, Shafie SR, Bahari H, Abdullah MA (2020) Mikania micrantha extract inhibits HMG-CoA reductase and ACAT2 and ameliorates hypercholesterolemia and lipid peroxidation in high cholesterol-fed rats. Nutrients 12:3077

James TW, Crockett SD (2018) Management of acute pancreatitis in the first 72 hours. Curr Opin Gastroenterol 34:330–335

Lee PJ, Papachristou GI (2019) New insights into acute pancreatitis. Nat Rev Gastroenterol Hepatol 16:479–496

Li H, Lin Y, Zhang L, Zhao J, Li P (2022) Ferroptosis and its emerging roles in acute pancreatitis. Chin Med J (engl) 135:2026–2034

Lin TY, Zhang YF, Wang Y, Liu Y, Xu J, Liu YL (2022) NAFLD aggravates acute pancreatitis through bacterial translocation and cholesterol metabolic dysregulation in the liver and pancreas in mice. Hepatobiliary Pancreat Dis Int 22:504–511

Liu Z, Gomez CR, Espinoza I, Le TPT, Shenoy V, Zhou X (2022) Correlation of cholesteryl ester metabolism to pathogenesis, progression and disparities in colorectal cancer. Lipids Health Dis 21:22

Llaverias G, Laguna JC, Alegret M (2003) Pharmacology of the ACAT inhibitor avasimibe (CI-1011). Cardiovasc Drug Rev 21:33–50

Ma X, Dong X, Xu Y, Ma N, Wei M, Xie X, Lu Y, Cao W, Lu G, Li W (2022) Identification of AP-1 as a critical regulator of glutathione peroxidase 4 (GPX4) transcriptional suppression and acinar cell ferroptosis in acute pancreatitis. Antioxidants (Basel) 12:100

Mauri M, Calmarza P, Ibarretxe D (2021) Dyslipemias and pregnancy, an update. Clin Investig Arterioscler 33:41–52

Ohtawa M, Arima S, Ichida N, Terayama T, Ohno H, Yamazaki T, Ohshiro T, Sato N, Omura S, Tomoda H, Nagamitsu T (2018) Design and synthesis of A-ring simplified pyripyropene A analogues as potent and selective synthetic SOAT2 inhibitors. ChemMedChem 13:411–421

Pramfalk C, Ahmed O, Pedrelli M, Minniti ME, Luquet S, Denis RG, Olin M, Hardfeldt J, Vedin LL, Steffensen KR, Ryden M, Hodson L, Eriksson M, Parini P (2022) Soat2 ties cholesterol metabolism to beta-oxidation and glucose tolerance in male mice. J Intern Med 292:296–307

Raal FJ, Marais AD, Klepack E, Lovalvo J, McLain R, Heinonen T (2003) Avasimibe, an ACAT inhibitor, enhances the lipid lowering effect of atorvastatin in subjects with homozygous familial hypercholesterolemia. Atherosclerosis 171:273–279

Schepers NJ, Bakker OJ, Besselink MG, Ahmed Ali U, Bollen TL, Gooszen HG, van Santvoort HC, Bruno MJ, Dutch Pancreatitis Study G (2019) Impact of characteristics of organ failure and infected necrosis on mortality in necrotising pancreatitis. Gut 68:1044–1051

Shen Z, Wang X, Zhen Z, Wang Y, Sun P (2021) Metabolic syndrome components and acute pancreatitis: a case-control study in China. BMC Gastroenterol 21:17

Wang YJ, Bian Y, Luo J, Lu M, Xiong Y, Guo SY, Yin HY, Lin X, Li Q, Chang CCY, Chang TY, Li BL, Song BL (2017) Cholesterol and fatty acids regulate cysteine ubiquitylation of ACAT2 through competitive oxidation. Nat Cell Biol 19:808–819

Withanage MHH, Liang H, Zeng E (2022) RNA-Seq experiment and data analysis. Methods Mol Biol 2418:405–424

Xiao AY, Tan ML, Wu LM, Asrani VM, Windsor JA, Yadav D, Petrov MS (2016) Global incidence and mortality of pancreatic diseases: a systematic review, meta-analysis, and meta-regression of population-based cohort studies. Lancet Gastroenterol Hepatol 1:45–55

Xu H, Zhou S, Tang Q, Xia H, Bi F (2020) Cholesterol metabolism: new functions and therapeutic approaches in cancer. Biochim Biophys Acta Rev Cancer 1874:188394

Zhou Z, Liang S, Zhou Z, Liu J, Meng X, Zou F, Yu C, Cai S (2022) Avasimibe alleviates disruption of the airway epithelial barrier by suppressing the Wnt/beta-catenin signaling pathway. Front Pharmacol 13:795934